Original Research Article

The vacancy energy in metals: Cu, Ag, Ni, Pt, Au, Pd, Ir and Rh

ABSTRACT

The predictive calculations of vacancy formation energies in metals: Cu, Ag, Ni, Pt, Au, Pd, Ir and Rh are presented. The energy is given as a function of electron density. Density functional theory underestimates the vacancy formation energy when structural relaxation is included. The unrelaxed mono-vacancy formation, unrelaxed di-vacancy formation, unrelaxed di-vacancy binding and low index surface energies of the fcc transition metals Cu, Ag, Ni, Pt, Au, Pd, Ir and Rh has been calculated using embedded atom method. The values for the vacancy formation energies agree with the experimental value. We also calculate the elastic constants of the metals and the heat of solution for the binary alloys of the selected metals. The average surface energies calculated by including the crystal angle between planes (hkl) and (111) correspond to the experiment for Cu, Ag, Ni, Pt and Pd. The calculated mono-vacancy formation energies are in reasonable agreement with available experimental values for Cu, Ag, Au and Rh. The values are higher for Pt and Ir while smaller values were recorded for Ni and Pd. The unrelaxed di-vacancy binding energy calculated agrees with available experimental values in the case of Cu, Ni, Pt and Au.

Keywords: EAM; Energy calculations; Elastic constants; Heats of solutions.

UNDER PEER REVIEW

INTRODUCTION

Many stories have been expended on the interatomic potential models competent for computer simulation of metallic systems. Out of many intend methods so far, the embedded-atom method (EAM) is an extensively used technique proposed (Daw et al., 1983) for the understanding of many-body potential models for material. Using the EAM, the energy need to position a trivial impurity atom in a lattice is taken as a function of the electron density at that peculiar site. Each atom species at that site therefore has an unmatched energy function of the electron density (Puska et al., 1981). Through this belief, many authors have originated several potential models. Finnis and Sinclair, 1984 developed a model which is mathematically analogous to the EAM. The functional form of the energy of the EAM was deduce (Manninen, 1986) and (Jacobson et al., 1987) using density-functional theory. By replacing the atomic electron density with an exponentially decline function, Johnson (1988) developed a simple analytic model for fcc (face-centered cubic) metals using nearest neighbor distance. This EAM function is sufficient only for nearest-neighbor interaction. The relevancy of Johson analytic EAM has been proof by calculating the ground state properties of some chosen metals.

The exponential form for absolute charge density has empowered Mei et al., 1990 to procure a closet analytic form of embedding function. By chosen exponential charge density of interest, they obtained potential parameters for fcc metals using a third neighbor model. Cai and Ye, 1996 developed the EAM potential under the assumption that the embedding energy is supposed to be of the total form present by Banerjea and Smith (1988).

It is now open that everyone have choice of potentials and embedding energy but the most significant ones are those that can portray the significant parameters of the metals and alloys.

UNDER PEER REVIEW

The employed potential utilized the total form of the embedded function present by Mayer with two-body potential given by Rose et al., 1984. This potential function was select for it is very simple form and is easy to be used in computer simulation. The potential parameters of this model are decided by fitting lattice constant, three elastic constants (C11, C12, C44), cohesive energy, and vacancy forming energy using an optimization technique. The procure parameters have been used to calculate properties including bulk modulus, monovacancy forming energy, divacancy forming energy, divacancy binding energy, the surface energy of the low index crystal, and the elastic constants. Information concerning the ground state properties of these metals is significant in mandate to know the kind of materials that can be formed from such metals. Zhang and Liu (2002) developed an embedded atom method potential for Ni-Al alloys. Their declaration of the embedded function was devise in analogy with the density function theory. Consistent empirical embedded-atom potential that contains a long range force for fcc metals and alloys has been developed to estimate the elastic constants and the heats of solution of some choice fcc metals (Iyad, 2009). In this scene, each atom in the metal is fixed into the electron gas produce by the other atoms.

The total energy of EAM is given as

$$E_{tot} = \sum_i F_i(\rho_i) + \frac{1}{2}\sum_{i,j} \phi_{ij}(r_{ij}) \qquad (1)$$

where

$$\rho_i = \sum_{j \neq i} f_{ij}(r_{ij}) \qquad (2)$$

The parameter $F_i(\rho_i)$ is the energy to embed an atom into the local compactness of the remaining atoms, ϕ_{ij} is an electrostatic two-body interaction between atoms i and j and $f_{ij}(r_{ij})$ is the local electron density, ρ is the host electron density. So far, equation (1) features three important functions which are $F(\rho)$, $\rho(r)$ and $\phi(r)$.

UNDER PEER REVIEW

THEORY

In the Analytic Embedded Atom Method, the electron density is given by:

$$f(r) = f_e exp\left[-\beta\left(\frac{r}{r_o} - 1\right)\right] \quad (3)$$

The embedding potential between atom i and atom j is given by:

$$\phi^{ij}(r) = \phi_e exp\left[-\gamma\left(\frac{r}{r_o} - 1\right)\right] \quad (4)$$

The embedding function is determined using equation (5):

$$F(\rho) = -E_c\left[1 - \frac{\alpha}{\beta} ln\left(\frac{\rho}{\rho_o}\right)\right]\left[\frac{\rho}{\rho_o}\right]^{\frac{\alpha}{\beta}} - \Phi_e\left[\frac{\rho}{\rho_o}\right]^{\frac{\gamma}{\beta}} \quad (5)$$

where $\rho_o = 12 f_e$ and $\Phi_e = 6\phi_e$

To determine the two adjustable parameters f_e and ϕ_e for each metal, equation (6) was used.

$$f_e = \frac{SE_c}{\Omega_e} \text{ and } \phi_e = \frac{E_c}{6} \quad (6)$$

where S is an arbitrary scaling constant.

The parameters α, β and γ can easily be determined from equations (7 – 9).

$$\alpha = 3\left(\frac{\Omega_e B}{E_c}\right)^{\frac{1}{2}} \quad (7)$$

$$\beta = \left(\frac{15E_c\Omega_e G}{E_v(E_v+E_c)}\right)^{\frac{1}{2}} \quad (8)$$

$$\gamma = \left(\frac{15\Omega_e G(E_c+E_v)}{E_c E_v}\right)^{\frac{1}{2}} \quad (9)$$

The elastic constants C_{11}, C_{12} and C_{44}, were calculated using equations (10), (11) and (12):

$$C_{11} = \frac{a_o^2}{2\Omega_e}\left[\left\{\varphi_e''(r) - \frac{1}{r_o}\varphi_e'(r)\right\} + 2F'(\rho_e)\left\{f_e''(r) - \frac{1}{r_o}f_e'(r)\right\}\right] \quad (10)$$

UNDER PEER REVIEW

$$C_{12} = \frac{a_o^2}{4\Omega_e}\left[\left\{\varphi_e''(r) - \frac{1}{r_o}\varphi_e'(r)\right\} + 2F'(\rho_e)\left\{f_e''(r) - \frac{1}{r_o}f_e'(r)\right\}\right] + \frac{8a_o^2}{\Omega_e}\left(f_e'(r)\right)^2 F''(\rho_e) \quad (11)$$

$$C_{44} = \frac{a_o^2}{4\Omega_e}\left[\left\{\varphi_e''(r) - \frac{1}{r_o}\varphi_e'(r)\right\} + 2F'(\rho_e)\left\{f_e''(r) - \frac{1}{r_o}f_e'(r)\right\}\right] \quad (12)$$

The bulk modulus B and the shear modulus G, in equations (7 – 9) is determined from equations (13) and (14) respectively.

$$B = \frac{1}{3}(C_{11} + 2C_{12}) \quad (13)$$

$$G = \frac{1}{5}(C_{11} - C_{12} + 3C_{44}) \quad (14)$$

Energy Calculations:

Vacancy migration which most often leads to vacancy forming is the controlling movement behind atomic carriage in most elemental crystals, and is of underlying consequence in procedure similar solid phase transformations and fault migration. Vacancy formation implies the removal of an atom from the interior of a crystal. The twelve two-body bonds were removed; the embedding energy at the equilibrium electron density is removed and the mono-vacancy formation energy is rate at equilibrium electron density. The unrelaxed mono-vacancy formation energy is calculated using equations (15) and (16)

$$E_{1v}^{uf} = -12F(\rho_e) + 12F\left(\frac{11}{12}\rho_e\right) - 6\phi_e \quad (15)$$

$$E_{1v}^{uf} = -12E_n + 12E_{n-1} \quad (16)$$

where E_n is the total energy of the system having no vacancy.

The unrelaxed di-vacancy formation energy can be computed using equation (17)

$$E_{2v}^{uF} = -18E_n + 14E_{n-1} + 4E_{n-2} \quad (17)$$

The unrelaxed di-vacancy binding energy is calculated using:

$$E_{2v}^{uB} = 2E_{1v}^{uf} - E_{2v}^{uf} = -6E_n + 10E_{n-1} - 4E_{n-2} \quad (18)$$

UNDER PEER REVIEW

The low index surface energy can be computed with equations (19) to (20):

The number of bonds broken on (111) surface $= (3\ bonds/atom)\text{x}\ (1atom/unit\ cell)$

Therefore number of bonds broken on (111) surface = $3/(\frac{\sqrt{3}}{4}a_o^2)$

$E_{surf} = E_{12-3} = E_9\ ;\ E_{bulk} = E_n = E_{12}$

$\Gamma_{111}^U = N_s/A(E_9 - E_{12})$

where N_s is the number of atom on the surface.

$$\Gamma_{111}^U = \frac{4}{a_o^2\sqrt{3}}(E_9 - E_{12}) \quad (19)$$

Similarly for Γ_{100}^U and Γ_{110}^U we have

$$\Gamma_{100}^U = \frac{2}{a_o^2}(E_8 - E_{12}) \quad (20)$$

$$\Gamma_{110}^U = \frac{\sqrt{2}}{a_o^2}(E_7 + E_{11} - 2E_{12}) \quad (21)$$

The crystal angle between planes (*hkl*) and (111) is calculated using

$$cos\theta_{(hlk)} = \frac{(h+l+k)}{\sqrt{3(h^2+k^2+l^2)}} \quad (22)$$

Alloy potentials and heats of solutions

In computing the alloys pair potentials, the mixing rule in equation (23) was used

$$\phi^{ab}(r) = \frac{1}{2}\left[\frac{f^a(r)}{f^b(r)}\phi^{aa}(r) + \frac{f^b(r)}{f^a(r)}\phi^{bb}(r)\right] \quad (23)$$

and the heats of solution for atom type-*b* as an impurity and atom type-*a* as the host is computed by the summation of equations (24 – 29).

Remove host : $\Delta H_1 = -F^a(\rho_e^a) - \sum \phi^{aa}(r_e^a)$ (24)

UNDER PEER REVIEW

Add impurity : $\Delta H_2 = + F^a(\rho_e^a) + \sum \phi^{ab}(r_e^a)$ (25)

Adjust neighbours: $\Delta H_3 = - \sum F^a(\rho_e^a) + \sum F^a(X)$ (26)

where $X = \rho_e^a + \Delta\rho$ (27)

and $\Delta\rho = - f^a(r_e^a) + f^b(r_e^a)$ (28)

Adjust cohesive energy: $\Delta H_4 = - E_c^a + E_c^b$ (29)

Hence, $\Delta H = \Delta H_1 + \Delta H_2 + \Delta H_3 + \Delta H_4$ (31)

It is essential to include lattice relaxations in many calculations involving energies [1]. The relaxation energy is given as:

$$\Delta H_r = -\left[1.1\delta 7\left(\frac{\Omega_{ea}}{\Omega_{eb}} - 1\right)\right]^2 \quad (32)$$

Here, ρ_e^a is the equilibrium electron density of *a*–type atoms,

Ω_{ea} is the atomic volume of *a* - type atoms and

Ω_{eb} is the atomic volume of b - type atoms.

UNDER PEER REVIEW

Table 1.0: Experimental data used in fitting procedure consists of equilibrium lattice constants (a_o), cohesive energy E_c, vacancy formation energy E_{1v}^{uf} and the elastic constants: (C_{11}, C_{12}, C_{44} in $ergcm^{-3}$(column 5 - 7)) and $eV/\text{Å}^3$ (column 8 – 10). The elastic constants: C_{11}, C_{12}, C_{44} in the last three column was converted from $ergcm^{-3}$ to $eV/\text{Å}^3$.

S/N	Atom	)								
1	Cu	3.615[a]	3.54[c]	1.30[h]	1.670[a]	1.240[a]	0.760[a]	1.04	0.77	0.47
2	Ag	4.090[a]	2.85[c]	1.10[h]	1.240[b]	0.934[b]	0.461[b]	0.77	0.58	0.29
3	Ni	3.520[a]	4.45[c]	1.70[i]	2.465[b]	1.473[b]	1.247[b]	1.54	0.92	0.78
4	Pt	3.920[a]	5.77[c]	1.60[i]	3.470[b]	2.510[b]	0.765[b]	2.17	1.57	0.48
5	Au	4.080[c]	3.93[c]	0.90[h]	1.860[b]	1.570[b]	0.420[b]	1.16	0.98	0.26
6	Pd	3.890[c]	3.91[c]	1.54[i]	2.341[b]	1.760[b]	0.712[b]	1.46	1.10	0.44
7	Ir	3.840[c]	6.94[c]	1.80[d]	5.990[b]	2.560[b]	2.690[b]	3.74	1.60	1.68
8	Rh	3.800[c]	5.75[c]	1.71[g]	4.220[b]	1.920[b]	1.940[b]	2.63	1.20	1.21

Refs: [a](Folies *et al*., 1986) ; [b](Simmons and Wang, 1971); [c](Kittel, 1996); [d](Landolt-Börnstein, 1991) ; [e](Ziesche and Perdew, 1994); [f](Sisoda and Verma, 1989) ; [g](De Boer *et al.*, 1988); [h](Ballufi, 1978); [i](Johnson, 1989); [j](Ghorai, 1991).

UNDER PEER REVIEW

RESULTS AND DISCUSSION

Table 2.0 : Calculated input parameters Ω_e, B, G and model parameters $f_e, \varphi_e, \alpha, \beta$ and γ

S/N	Metal	Ω(Å^3)	B(eV/Å^3)	G(eV/Å^3)	f_e (eV)	φ_e (eV)	$\frac{\varphi_e}{\alpha}$	$\frac{\gamma}{\beta}$	γ
1	Cu	11.81	0.86	0.34	0.30	0.59	5.09	5.81	7.94
2	Ag	17.10	0.65	0.21	0.17	0.47	5.91	5.96	8.26
3	Ni	10.90	1.13	0.59	0.41	0.74	4.98	6.41	8.86
4	Pt	15.06	1.77	0.41	0.38	0.96	6.44	6.70	8.56
5	Au	16.98	1.04	0.19	0.23	0.66	6.36	6.67	8.20
6	Pd	14.72	1.22	0.34	0.27	0.65	6.43	5.90	8.23
7	Ir	14.16	2.31	1.44	0.49	1.16	6.51	10.98	14.09
8	Rh	13.72	1.68	1.01	0.42	0.96	6.00	12.05	14.54

UNDER PEER REVIEW

Table 3.0: Calculated formation $E_{2v}^{uF}(eV)$, binding $E_{2v}^{uB}(eV)$, and low index surface$\Gamma_{(hlk)}^{U}(\frac{ergs}{cm^2})$ energies. The present work is listed first (values with asterisk include $cos\theta_{(hlk)}$). The experimental values are listed second, and the results of other authors are listed last.

S/N	Atom	$E_{2v}^{uF}(eV)$	$E_{2v}^{uB}(eV)$	$E_{1v}^{uF}(eV)$	$\Gamma_{(11)\times10^{-3}}$	$\Gamma_{(10)\times10^{-3}}$	$\Gamma_{(10)\times10^{-3}}$	$\Gamma_{(hk)\times10^{-3}}$
1	Cu	2.41	0.19 0.13 ± 0.04^{l} , 0.3^{m} 0.27^{a}	1.31 1.3^{h} 1.28^{a}	1.02, 1.02*	1.23, 2.14*	1.34, 1.64*	1.20, 1.60 1.77^{q} 1.28^{a}, 1.57^{q}
2	Ag	2.13	0.15 0.38^{n} 0.22^{a}	1.14 1.10^{h}	0.70, 0.70*	0.86, 1.49*	0.94, 1.15*	0.83, 1.11 1.32^{q} 0.70^{a}, 1.19^{q}
3	Ni	3.15 $2.92–3.10^{a*}$	0.27 0.33^{p}, 0.28^{l*} 0.44^{a}	1.71 1.80^{d}	1.32, 1.32*	1.56, 2.71*	1.69, 2.06*	1.52, 2.03 2.24^{q}
4	Pt	3.29	0.19 $0.1 – 0.2^{h}$ 0.45^{a}	1.74 1.60^{i}	1.24, 1.24*	1.56, 2.70*	1.72, 2.10*	1.51, 2.02 2.50^{**} 1.61^{a}, 1.99^{q}
5	Au	1.93	0.09 0.1 ± 0.03^{r},0.3^{t} 0.22^{a}	1.01 0.90^{h}	0.70, 0.70*	0.89, 1.54*	0.99, 1.21*	0.88, 1.15 1.54^{q} 0.90^{a}, 1.03^{q}
6	Pd	3.10	0.20 0.34^{a}	1.65 1.70^{i}	1.15, 1.15*	1.41, 2.45*	1.54, 1.89*	1.37, 1.82 2.00^{**} 1.36^{a}, 1.57^{q}
7	Ir	3.64	0.32	1.98 1.80^{d}	1.25, 1.25*	1.47, 2.54*	1.58, 1.93*	1.43, 1.91 3.00^{**} 2.84^{a}
8	Rh	3.14	0.28	1.71 1.71^{g}	0.78, 0.78*	0.91, 1.58*	0.98, 1.20*	1.28, 1.72 2.60^{**}

Refs: [a](Folies *et al*., 1986) ; [d](Landolt-Börnstein, 1991) ; [e](Ziesche and Perdew, 1994); [g](Ledbetter and Kim, 2001) ; [h](Ballufi, 1978); [i](Johnson, 1989) ; [j](Ghorai, 1991) ; [l](Seeger *et al*., 1963); [l*](Seeger and Schumacher, 1967) ; [m](Fluss *et al*., 1980); [n](Kraftmakher and Strelkov, 1970) ; [p](Mehrer *et al*., 1965) ; [q](Baskes, 1992); [r](Bauerle and Koehler, 1957); [t](Meshii *et al*., 1962) ; [u](Ehrhart *et al*., 1991); [a*](Nanao *et al*., 1977).

The calculated surface energies for the low index crystal faces are compared to the experimental polycrystalline average values (eV/cm^2). The experimental polycrystalline average values (last

UNDER PEER REVIEW

row) are accurate at least to about 10% and in a number of cases, indicated by an asterisk, have been crudely extrapolated from the melt temperature to 0K (Baskes, 1992).

Table 4.0: Calculated and experimental properties of pure metals. The first lines present the experimental values of elastic constants in $eV/Å^3$ (column 3 – 5) and Bulk modulus in $eV/Å^3$ (column 6). The second lines present the predicted values using common cut-off radius $1.11r_e \geq r_c \leq 1.25r_e$.

S/N	Metal				
1	Cu	1.04[a] 1.03	0.77[a] 0.57	0.47[a] 0.53	0.86[g] 0.72
2	Ag	0.77[b] 0.77	0.58[b] 0.43	0.29[b] 0.40	0.60[g] 0.54
3	Ni	1.54[b] 1.53	0.92[b] 0.84	0.78[b] 0.79	1.16[g] 1.07
4	Pt	2.17[b] 1.87	1.57[b] 1.02	0.48[b] 0.96	1.77[g] 1.30
5	Au	1.16[b] 1.18	0.98[b] 0.65	0.26[b] 0.61	1.08[g] 0.83
6	Pd	1.46[b] 1.66	1.10[b] 0.97	0.44[b] 0.88	1.21[g] 1.20
7	Ir	3.74[b] 3.72	1.60[b] 1.97	1.68[b] 1.90	2.22[b] 2.55
8	Rh	2.63[b] 2.53	1.20[b] 1.33	1.21[b] 1.28	1.68[*] 1.78

Refs: [a](Folies *et al*., 1986); [b](Simmons and Wang, 1971) ; [d](Landolt-Börnstein, 1991) ; [f](Sisoda and Verma, 1989) ; [g](De Boer *et al.*, 1988) ; [*]Computed using equation (8)

UNDER PEER REVIEW

Impurity	Host							
	Cu	Ag	Ni	Pt	Au	Pd	Ir	Rh
Cu		0.40 0.27 0.25[v]	0.11 0.10 0.11[v]	-0.19 -0.26 -0.30[v]	0.05 -0.08 -0.13[v]	0.10 0.05 -0.39[v]	-0.29 -0.33 -0.64[q]	-0.17 -0.20 -0.72[q]
Ag	0.79 0.52 0.39[v]		1.88 1.44	0.65 0.63	-0.06 -0.06 -0.16[v]	0.32 0.28 -0.11[v]	1.37 1.31 0.78[q]	1.12 1.02
Ni	0.08 0.07 0.03[v]	0.75 0.57		-0.12 -0.23 -0.33[v]	0.33 0.19 0.22[v]	0.22 0.21 -0.09[v]	-0.34 -0.41 -0.25[q]	-0.14 -0.20 -0.35[q]
Pt	-0.30 -0.40 -0.53[v]	0.66 0.64	-0.23 -0.43 -0.28[v]		0.46 0.46	-0.03 -0.03	0.17 0.16	0.02 0.01
Au	-0.01 -0.27 -0.19[v]	-0.03 -0.03 -0.19[v]	0.84 0.42 0.28[v]	0.58 0.56		-0.03 -0.06 -0.20[v]	1.47 1.42 0.57[q]	0.91 0.84 0.37[q]
Pd	0.15 0.06 -0.44[v]	0.30 0.28 -0.29[v]	0.69 0.53 0.06[v]	-0.01 -0.01	0.01 -0.01 -0.36[v]		0.43 0.43	0.26 0.25
Ir	-0.94 -0.99 -0.73[q]	0.66 0.62 0.55[q]	-1.29 -1.41 -0.68[q]	0.07 0.06	0.51 0.47 0.38[q]	-0.06 -0.06 -0.28[q]	-	0.004 0.006
Rh	-0.44 -0.48 -0.74[q]	0.52 0.47 0.35[q]	-0.47 -0.56 -0.55[q]	-0.01 -0.00	0.32 0.27 0.24[x]	0.03 0.03 -0.35[q]	-0.04 -0.04	-

Table 5.0: Heats of solution for the likely binary alloys of the chosen fcc metals. The results of the unrelaxed calculations are listed first, the values with relaxation second, the experimental values (Ref. v and w) where valid, and the adapted values from other author (Ref. q and y) are listed last.

Refs: [q](Baskes, 1992); [w](Miedema *et al*., 1980) ; [v](Hultgren *et al*., 1973) ; [y](Iyad, 2009)

UNDER PEER REVIEW

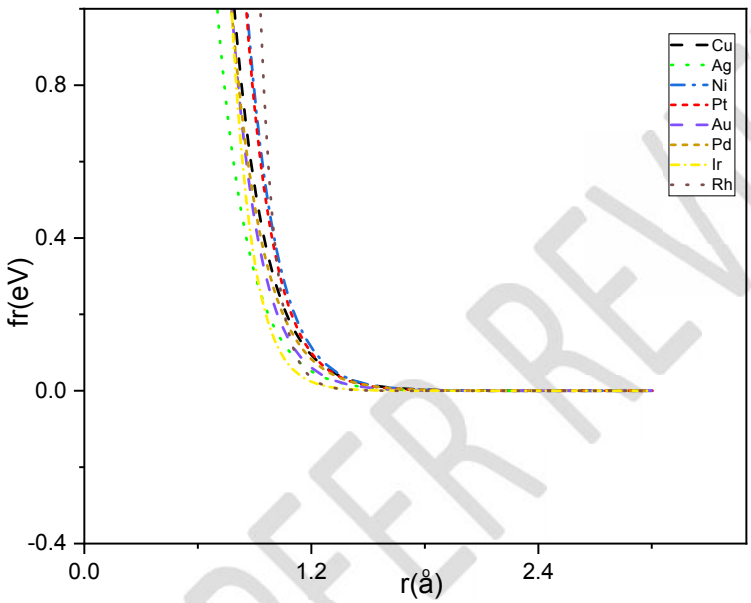

Fig.1: Characteristics of the electron density function for the selected metals.

UNDER PEER REVIEW

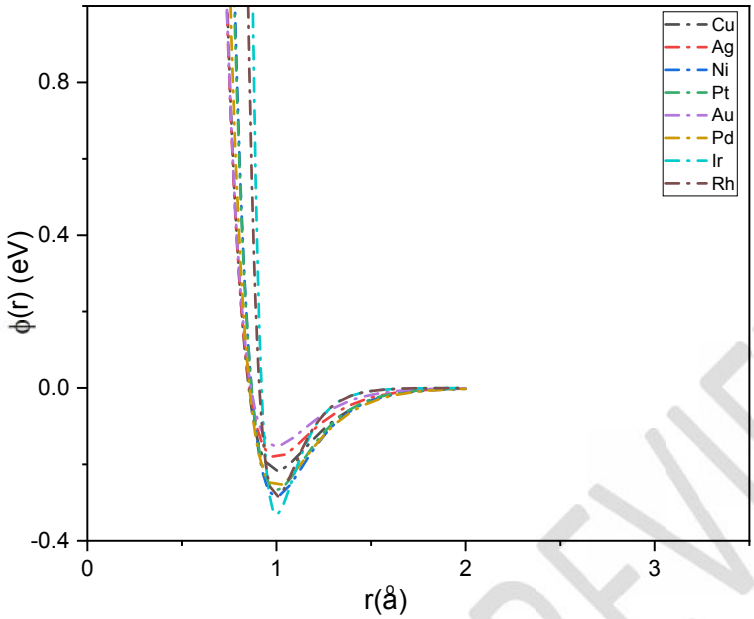

Fig. 2: Characteristics of the pair-potential function for the selected metals.

UNDER PEER REVIEW

Fig. 3: Characteristics of the embedding energy function for the selected metals.

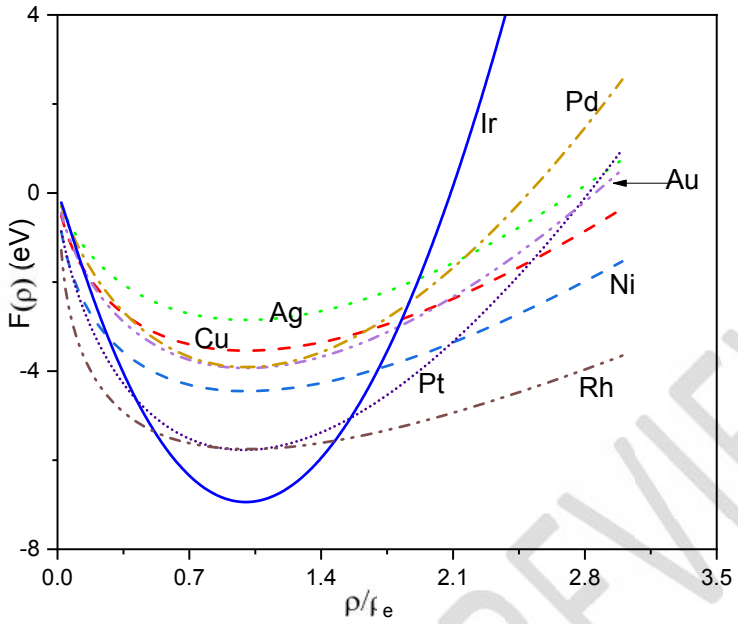

Fig. 3: Characteristics of the embedding energy function for the selected metals.

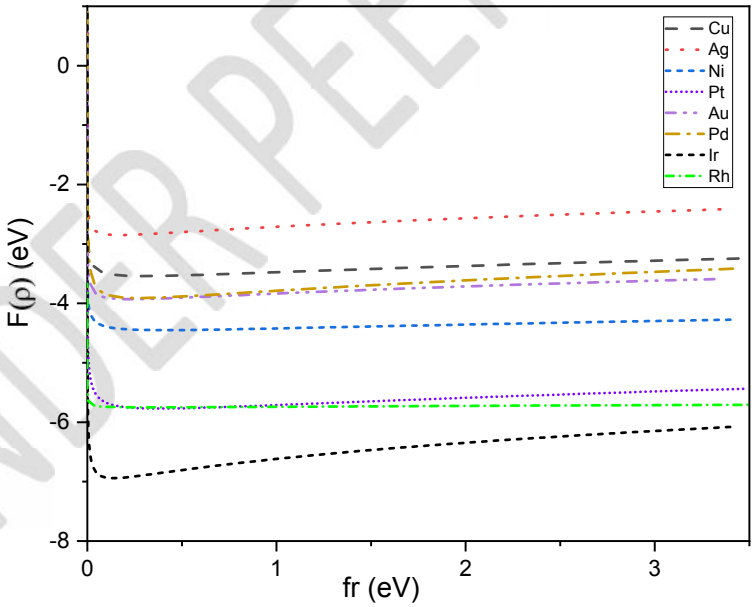

Fig. 4: Characteristics of the embedding energy function with electron density for the selected metals.

UNDER PEER REVIEW

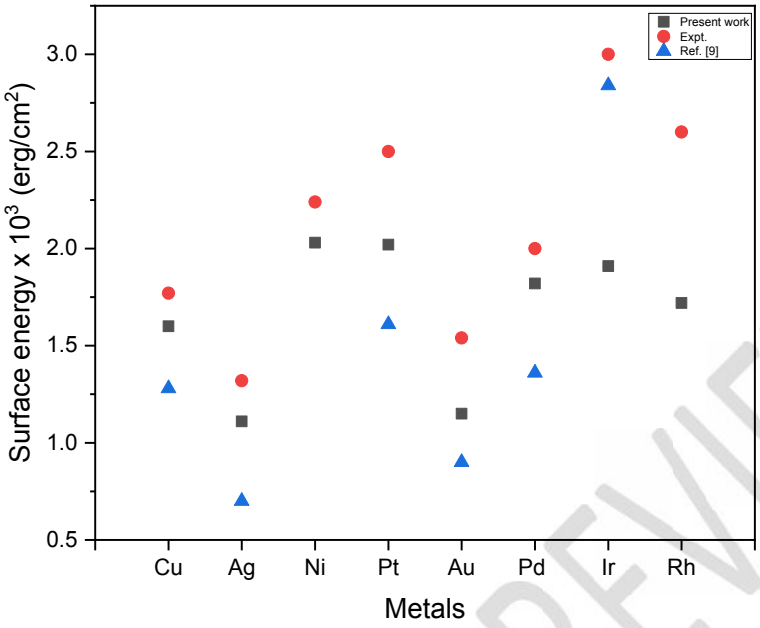

Fig. 5: Plot of unrelaxed surface energies for the selected metals.

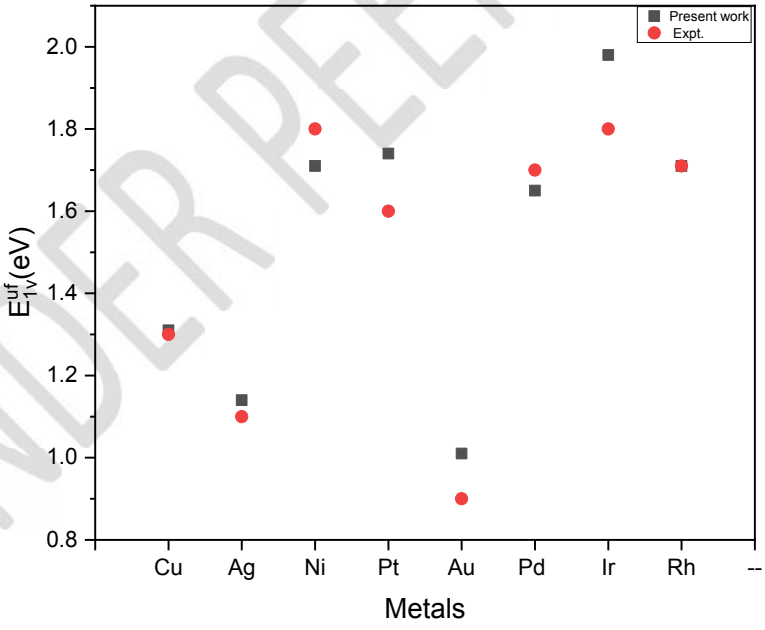

Fig. 6: Plot of unrelaxed mono-vacancy formation energies for the selected metals.

UNDER PEER REVIEW

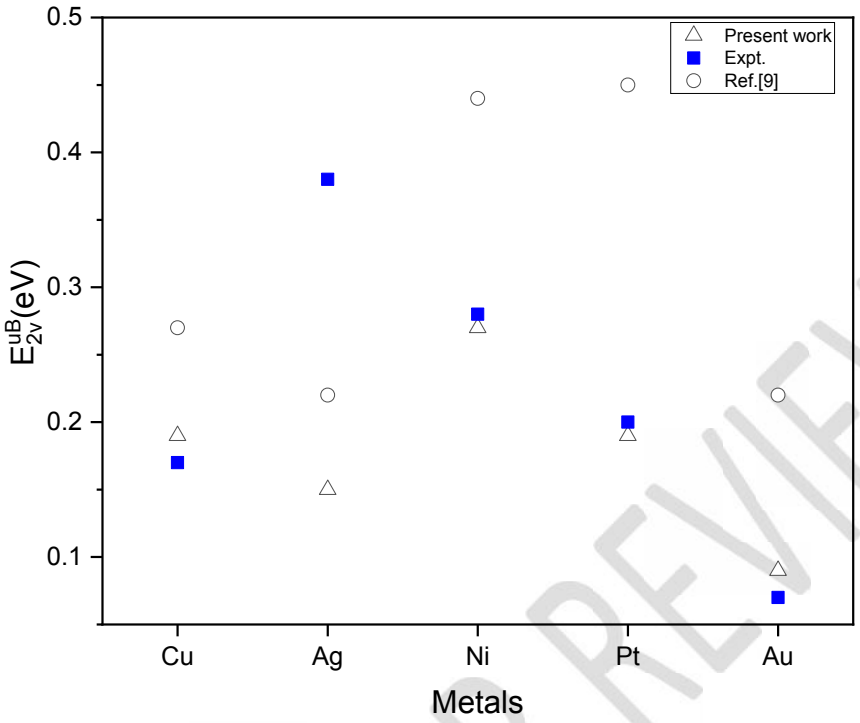

Fig. 7: Plot of unrelaxed di-vacancy binding energies for some of the selected metals.

In Fig.1, the electron density $f(r)$ displays the common characteristics for the selected metals.

Fig. 2 shows the least (minimum) free energy curves for the electron which gives the equilibrium interatomic distance. The width of the curves increases as the values of *r* increases, therefore the position of the principal minimum is displaced to larger values of *r*. The pair-potential tends to group Cu, Ag, Ni, Pt, Au and Pd, also Ir and Rh.

In Fig. 3, there are systematic trends in the embedding energies. The curvature of the embedding function accounts for the "many-body" aspect of the model with the least embedding energy occurring for Ir.

Fig. 4. shows that the embedding function goes through the appropriate range of electron densities and the characteristics curves tends to group: Cu, Pd with Au and also Pt with Rh.

UNDER PEER REVIEW

Fig. 5. presents the unrelaxed surface energies for the selected metals while Fig. 6 and Fig. 7 give the plots of the unrelaxed mono-vacancy formation and di-vacancy binding energies respectively.

The properties calculated in this work will help in finding new metals/compounds for substitution in alloying processes. The ground state properties such as, surface energies, vacancy formation energies and heats of solutions has been calculated. The sensitivity of the heats of solutions on the embedding function and the potential produces good results in comparison with the available experimental values.

Finding new metals/compounds for substitution in alloying processes is an issue that needs to be addressed by the material scientist especially in this state of scarcity in the case of palladium. The calculated mono-vacancy formation energies are in reasonable agreement with available experimental values for Cu, Ag, Au and Rh as shown in Fig. 6. The values are higher for Pt and Ir while smaller values were recorded for Ni and Pd. The unrelaxed di-vacancy binding energy calculated agree with available experimental values closer than the results of Folies *et al*., 1986 in the case of Cu, Ni, Pt and Au (See Fig. 7).

The unrelaxed surface energy for the three fcc low-index planes was estimated by dividing the total energy increase in separating bulk material on a crystallographic plane by the total new surface area created. In all the cases, the trends $E_{(111)} < E_{(100)} < E_{(110)}$ was observed and also by including crystal angle between planes, we have $E_{(111)} < E_{(110)} < E_{(100)}$. The lowest surface energy corresponds to the closed-packed (111) plane as observed in Table 3.0. Therefore closed packed surfaces looks most stable for fcc metals. The calculated average surface energies are closer to the experimental values than those obtained by the MEAM (Baskes, 1992).

The average surface energies predicted low average values compared to the available experimental values but when the crystal angle was included, moderate average values were obtained and they

UNDER PEER REVIEW

are in good agreement with the available experimental values for Cu, Ag, Ni, Pt and Pd. The results for Cu, Pt, Au and Pd are closer to the experimental values than that of Ref. (Folies *et al*., 1986) (See Fig. 5) and (Baskes, 1992) (See Table 3.0).

SUMMARY

The calculated ground state properties for the pure metals include surface energies, mono-vacancy formation energies, di-vacancy formation energies, di-vacancy binding energies, elastic constants and their heats of solutions. The agreement between the experiment and the calculated values is quite good for the metals and their alloys. From the heats of solutions calculated (Table 5.0), the positive heats of solution recorded are higher than the negative heats of solutions. The most negative heats of solution occur for the relaxation values and most positive occurs for the unrelaxed values. The pair potential function of the alloy mixing '$\varphi(r)^{ab}$' between two different atoms *a* and *b* gives reasonable values of heats of solutions in the case of Cu, Ag, Au, Ni and Pt.

CONCLUSION

The EAM model was used to compute some ground state properties of the selected fcc transition metals and their binary alloys. The di-vacancy binding energies calculated also agree with the available experimental values. The surface energies predicted by the model was low in comparison to experiments but when the crystal angle was included, the model predicted low index surface energies that agree reasonably with the experiment in better comparison with the values from Ref. (Foiles *et al*., 1986) and (Baskes, 1992). The model is well-suited for studies of defects energies in metals and their alloys. The surface energies calculated by including the crystal angle between planes corresponds to the experiment for Cu, Ag, Ni, Pt and Pd. For surface energy minimization, it is good that the (111) texture should be favoured in an fcc film. The embedding function $F(\rho)$ with

UNDER PEER REVIEW

the angle between planes (*hkl*) and (111) can be used to estimate the relative values of surface energy for surfaces in different orientations.

REFERENCES

Ballufi RW. *J Nucl. Matter*. 1978, 69 & 70:240.

Banerjea A and Smith J.R. *Phys. Rev. B*. 1988, 37, 6632.

Baskes M I. *Phys. Rev B*. 1992; 46:2727.

Bauerle JE and Koehler JS. 1957. 107:1493.

Cai J. and Ye YY.: *Phys. Rev. B*. 1996, 54, 8398.

Daw MS, Bisson CL and Wilson WD. *Solid commun*. 1983; 46.

De Boer FR, Boom R, Mattens WCM, Miedema AR and Niessen AK. *Cohesion in Metals*, Vol. 1. Amsterdam: North Holland. 1988.

Ehrhart P, Jung P, Schultz H and Ullmaier H. Atomic Defects in Metals. *Springer Verlag.* Edited by Ullmaier .H. *Landolt-Börnstein*. New Series. Group III/25, Berlin; 1991.

Finnis MW and Sinclair JE. *Philos. Mag. A*. 1984, 50, 45.

Fluss MJ, Smedskjaer LC, Siegel RW, Longini DG and Chason MK. *J. Phys*. F. 1980,10:1763.

Foiles SM, Baskes MI and Daw MS. *Phys.Rev. B*. 1986, 33:7983.

Ghorai A. *Physica Status Solidi B.* 1991, 167:551.

Hultgren R, Desai PD, Hawkins DT, Gleiser M and Kelley KK. Selected Values of the Thermodynamic Properties of Binary Alloys (American Society for Metals, Metals Park,OH); 1973.

Iyad AH, Young P. *J. Mater. Sci. Technol*. 2009, 25:6.

Jacobson KW, N*Á*rskov JK and Puska J. *Phys. Rev. B*. 1987, 35, 7423.

Johnson RA. *Phys. Rev. B.* 1989, 39, 17:12554 – 12559.

Johnson RA. *Phys. Rev. B*. 1988, 37, 3924.

UNDER PEER REVIEW

Kittel C. Introduction to Solid State Physics. 7th Edition. John Willey & Sons. Inc., New York, Chicester, Brisbarne, Toronto, Singapore. 1996, 28 – 98.

Kraftmakher YA and Strelkov PG. In Vacancies and Interstitials in Metals, edited by Seeger A., Schumacher D, Schilling W and Diehl J. (North-Holland), Amsterdam. 1970, 59.

Landolt-Bӧrnstein. New Series, Vols. III-11 and III-18 Berlin: *Springer-Verlag*. 1991.

Ledbetter H and Kim S. Monocrystal Elastic Constants and Derived Properties of The Cubic and The Hexagonal Elements, in: Handbook of Elastic Properties of Solids, Liquids and Gases, Academic Press. 2001, Vol. 2.

Manninen M. *Phys. Rev. B*. 1986, 34, 8486.

Mehrer H, Kbonmuller H and Seeger H. *Phys. Stat. Sol*. 1965, 10:725.

Mei J, Devenport JW and Fernando G.W. *Phys. Rev. B*. 1990, 43, 4653.

Meshii M, Mori T and Kauffman JW. *Phys. Rev*. 1962, 185:1239.

Miedema AR, de`Chatel PF, de Boer FR . *Physica B*. 1980, 100:1.

Nanao S, Kuribayashi K, Tanigawa S and Doyama M. *J. Phys. F: Met. Phys.* 1977, 7:1403.

Puska J, Nieminen RM and Manninen M. *Phys. Rev. B*. 1981, 24, 3037.

Rose JH, Smith JR, Guinea F and Ferrante J. *Phys. Rev. B*. 1984, 29, 2963.

Seeger A, Gerold V, Chik KP and Ruhle M. *Phys. Letters.* Netherlands. 1963, 6:107.

Seeger A and Schumacher D. *Mater. Sci. Eng*. 1967, 2:31

Simmons G and Wang H. Single Crystal Elastic Constants and Calculated Aggregate Properties: A Handbook (MIT Press, Cambridge); 1971.

Sisoda P and Verma MP. Shear Moduli of Polycrystalline Cubic Elements. *J. Phys. Chem. Solids*. 1989, 50:223 – 224.

UNDER PEER REVIEW

Zhang RF and Liu BX. Proposed model for calculating the standard formation enthalpy of binary transition-metal systems. *Appl. Phys. Lett* 2002, 81, 1219–1221.

Ziesche P, Perdew JP and Fiolhais C. Spherical Voids in the Stabilized Jellium Model: Rigouruos Theorems and Pad; Representation of the Void-Formation Energy. *Phy. Rev. B*. 1994, 49:7916.

UNDER PEER REVIEW